Satellite Instrument Calibration Issues: experience gained from SSMIS

William Bell, Stephen English, Steve Swadley[1] and Graeme Kelly[2]

Met Office, FitzRoy Road, Exeter EX1 3PB, UK
william.bell@metoffice.gov.uk, stephen.english@metoffice.gov.uk
[1]*Naval Research Laboratory, Monterey, CA 93943-5502 , USA*
[2] *ECMWF, Shinfield Park, Reading, RG2 9AX, UK*
steve.swadley@nrlmry.navy.mil,graeme.kelly@ecmwf.int

ABSTRACT

Following the launch of F16 SSMIS in October 2003, a number of instrumental biases have been investigated by the extended Cal/Val team. For the lower atmospheric temperature sounding channels, where radiometric performance is most critical for NWP data assimilation applications, the two most significant instrumental biases are associated with solar intrusions into the warm calibration load and thermal emission from the main reflector. Strategies have been developed at the Met Office and elsewhere to deal with these problems either through flagging or by correcting the measured brightness temperatures. A conservative Day 1 strategy has been implemented at the Met Office which involves flagging and subsequently rejecting intrusion affected observations, and correcting for reflector emission as part of a pre-processor. Pre-processed radiances for the low atmospheric sounding channels give global innovations in the range 0.2 - 0.3 K, and relatively stable biases, based on a short monitoring period (August - October 2005).

1 Introduction

The Special Sensor Microwave Imager/Sounder (SSMIS) is an important component of the US Defense Meteorological Satellite Program (DMSP). The instrument builds on the capabilities of its predecessor, the Special Sensor Microwave Imager (SSMI), which was launched on a series of platforms between 1987 and 1999 and continues to be an important data source for many NWP centres. SSMIS combines the imaging capabilities of SSMI with additional temperature and moisture sounding channels. The weighting functions of the temperature sounding channels (1-7 and 19-24) span the troposphere, stratosphere and lower mesosphere. This unique combination of capabilities in a single instrument makes SSMIS potentially very valuable for the assimilation of radiances in both clear and cloudy conditions.

SSMIS is the first conical scanning instrument to be used for temperature sounding and is seen by many as a testbed for the Conical Microwave Imager Sounder (CMIS) which will be an important component of the US NPOESS satellite system. The first SSMIS was launched on October 18th 2003 onboard DMSP F16 into a morning orbit (equatorial crossing time 20:13). Four further SSMIS are scheduled for launch between 2006 and 2012.

In terms of data quality, the requirements for radiances from temperature sounding channels for radiance assimilation are particularly stringent. The background equivalent radiance errors (given by $\mathbf{HBH}^{\mathbf{T}}$) from Met Office global forecasts at T+6 hours for SSMIS channels 2 - 7 are in the range 0.2 - 0.4K. In the Met Office 4D-Var assimilation system quality controlled and bias corrected clear sky radiances from AMSU-A give innovation statistics (standard deviations) in the range 0.14 - 0.20K for channels which peak in the troposphere. As a guideline therefore, it may be assumed that in order to improve the quality of the analysis and subsequently forecasts, innovations should have standard deviations of around 0.2K or better. The instrumental biases described here significantly increase the observed variance in the innovations from SSMIS. Initial evaluations gave standard deviations of 0.5 - 0.8K for the lower atmospheric sounding channels.

Following the launch of F16 SSMIS a number of anomalies in the performance of the instrument emerged, particularly for the temperature sounding channels. The most significant anomalies were associated with solar intrusions into the warm load used for the two point radiometric calibration and with emission from the main reflector which appears to have non zero emissivity. In section 2 these effects and the approaches used to characterise them are described. Section 3 outlines the strategy used to correct these effects and the overall approach to bias correction. Section 4 gives an indication of the resulting quality of the SSMIS radiances indicated by monitoring of the innovations. Section 5 briefly describes the longer term strategy for correcting these anomalies for F16 and the prospects for F17 SSMIS and beyond. Conclusions are given in Section 6.

2 Calibration Anomalies

During the Cal/Val phase two techniques have been particularly useful for investigating instrument problems: firstly, time series plots of innovations averaged over many scanlines and, secondly, a visualisation tool (DGS) which uses CAD engineering data together with orbit data to simulate the orientation of the spacecraft throughout orbit. Both tools have been used extensively in the investigation of the two most significant issues which are described in more detail below:

2.1 Solar Intrusions / Gain Anomalies

As the main off-axis paraboloidal reflector of SSMIS spins about the main axis of the instrument the Earth scene radiance is focussed onto feedhorns sited on the main instrument deck. Once per revolution (every 2 seconds) the feedhorns pass under the cold space reflector and the warm load. The warm load comprises high emissivity pyramidal structures (*tines*) maintained at a temperature close to 306 K. In this way, a two point radiometric calibration is obtained once per revolution (*ie* once per scan line) permitting the conversion of raw signal counts to antenna temperatures.

Figure 1 shows the evolution of the calibration parameters over the course of a six hour assimilation window spanning approximately three orbits. Also shown on the same scale is the evolution of the innovations for channel 6 (57.29 GHz). It can be seen that the anomalous spikes in the warm load counts causes positive anomalies in the gain which in turn correspond to negative departures in the innovations. Simulations with the visualisation package DGS showed that these anomalies corresponded to sections of the orbit where the warm load tines were subject to either direct solar illumination, or were subject to reflected solar illumination from the highly reflective main instrument deck. The effect of these solar intrusions is to warm the surface skin of the tines and causes an increase in the warm load counts, however the temperature sensors embedded deep in the substrate material do not respond to this superficial warming of the tines.

These intrusions generally occur four times per orbit, two reflected intrusions and two direct intrusions, with the former generally being more intense and of longer duration. The intensity and form of the intrusions varies throughout the year as a result of changes in the relative position of the sun and obscuration of the warm load by other structures on the platform. The strongest intrusions cause anomalous jumps in the innovations of magnitude 1 - 1.5 K for most of the temperature sounding channels.

2.2 Reflector Emission

The main reflector comprises a graphite epoxy honeycomb off-axis paraboloid coated with several sandwich layers of non-stoichiometric SiO_x and aluminium approximately 2 μm in thickness. Pre-launch tests indicated reflector reflectances of better than 0.9999, however due to significant launch delays (totalling 2 years) it is hypothesised that absorption of water by SiO_x resulted in significant degradation of reflectivity at microwave frequencies.

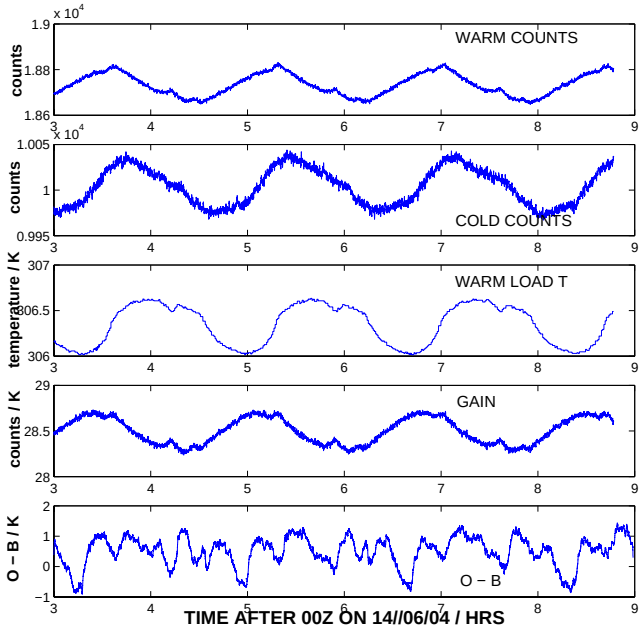

Figure 1: Radiometric calibration data for SSMIS and averaged innovations (O-B) for channel 6 (57.29GHz). The positive anomalies in the gain are correlated with negative anomalies in the innovations of magnitude 1 - 1.5K.

During each orbit SSMIS enters Earth shadow for a period of up to 30 minutes depending on the time of year. Immediately before entering Earth shadow and immediately after exiting Earth shadow the reflector is subject to solar illumination at near normal incidence (although the reflector is constantly rotating it is illuminated for a significant part of the rotation during these periods). A platinum resistance thermometer (PRT) mounted on the rim of the main reflector close to the support arm of the reflector records that the temperature drops to around 220K in Earth shadow and warms to approximately 300K over a period of 10 minutes following emergence from Earth shadow.

Figure 2 shows the scan averaged brightness temperatures alongside the evolution of the arm temperature. The magnitude of the discontinuity in innovations is 1.5 K for most of the lower atmospheric temperature sounding channels and up to 5K for the moisture sounding channels at 183 GHz.

2.3 Other Issues

In addition to these problems the Cal/Val team have investigated other issues including lunar intrusions in the cold space calibration view, banding in the upper atmospheric channels due to the calibration averaging scheme used, gain discontinuities in the 37 GHz channels and feedhorn dependant cross scan biases due to spacecraft obstruction of the earth view. Most of these problems are of secondary importance, or are dealt with easily using existing bias correction strategies and will not be described here in further detail.

3 Correction Strategies

This section describes the strategies employed to correct the systematic effects described above in the Met Office pre-processor. Different approaches have been used succesfully elsewhere and these are covered briefly in section 3.3. A two step approach has been adopted in the current Met Office system in which the intrusions and reflector emission are dealt with by the pre-processor, and residual cross scan biases and RT errors are

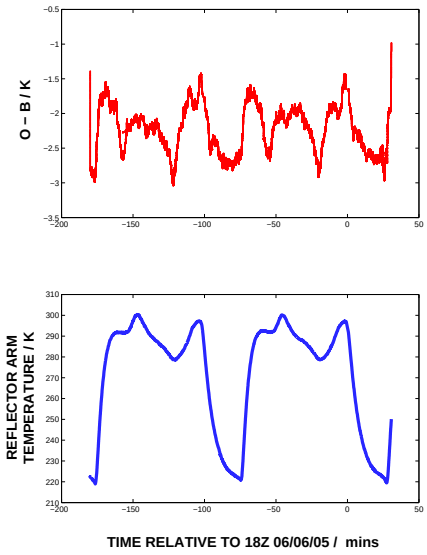

Figure 2: Time series of averaged innovations for channel 4 (top) and the evolution of the measured arm temperature (bottom). The rapid rise in arm temperature following emergence from Earth shadow (at T = -70 minutes) is accompanied by a sharp rise in the innovations.

corrected for using a predictor based scheme (Atkinson, 2005)

3.1 Flagging Solar Intrusions

As an initial Day 1 approach to pre-processing the SSMIS radiances at the Met Office it was decided that the solar intrusion affected observations should be flagged and thereafter rejected from the main 4D Var assimilation. Offline signal processing of time series of gains for channel 4 was used to identify the regions of the orbit affected by solar intrusions. These were used to build up a map in the space defined by the local solar zenith and azimuth angles. The performance is illustrated in Figure 3. Approximately 30 - 40 % of the data is flagged in this way.

3.2 Reflector Emission Correction

The scene temperature (T_{scene}) can be constructed from the observed brightness temperature (T_{obs}) as follows :

$$T_{scene} = \frac{T_{obs} - \varepsilon T_{ref}}{(1-\varepsilon)} \tag{1}$$

The unknowns to be determined are the temperature of the main reflector (T_{ref}) and the effective emissivity (ε) of the reflector for each channel. The emissivity is potentially frequency and polarisation dependent. From equation (1) the required accuracy in the determination of T_{ref} (ΔT_{ref}) and the emissivity ($\Delta\varepsilon$) to achieve a specified tolerable error in T_{scene} (ΔT_{scene}) can be computed. The results are summarised in Table 1.

Investigations showed that the measured arm temperatures are not sufficiently accurate estimates of the reflector temperature itself. Reflector emission corrections based on the arm temperature produced residuals of 0.5 K in innovations in the region of emergence from Earth shadow. An empirical reflector temperature was constructed from the measured arm temerature data as follows:

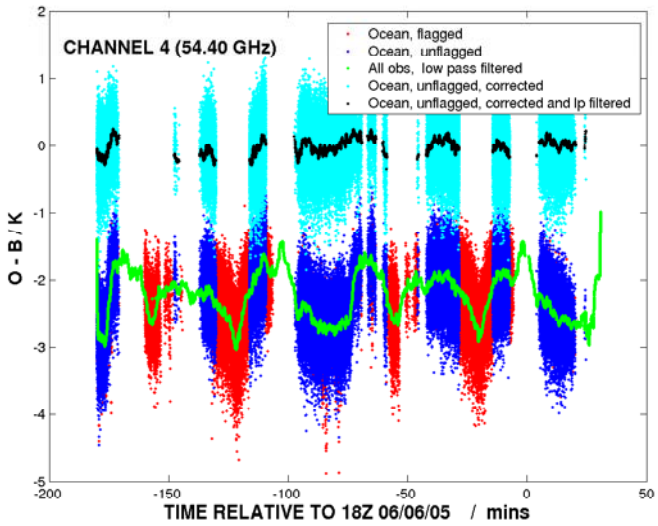

Figure 3: The performance of the intrusion flagging and antenna emission correction for channel 4 (54.4GHz). The green line shows the smoothed innovations for the uncorrected and unflagged data. The solid black line shows the averaged innovations of the data remaining after flagging and reflector emission correction

Channel	Frequency / GHz	Polarisation	ΔT_{scene} / K	ε_{nom}	$\Delta\varepsilon$	ΔT_{ref} / K
1 - 5	50.3 - 55.5	V	0.1	0.01	0.0008	10.0
6 - 7,19 - 24	57.3 - 63.3	LC	0.1	0.02	0.0010	5.0
9 - 11	183.31	H	0.5	0.04	0.0060	12.0
12 - 16	19.4 - 77.0	V/H	0.5	0.00	-	-

Table 1: Required accuracy in the estimate of reflector emissivity and temperature (ΔT_{ref} and $\Delta\varepsilon$) for a specified tolerable error in T_{scene} (ΔT_{scene}) using sensitivities computed from Equation 1 and assumed nominal emissivities

$$T_{ref}(t) = T_{arm}(t) + c\frac{dT_{arm}}{dt}(t) \tag{2}$$

Where the second term on the RHS can be thought of as a correction to the measured arm temperature. The derivative of the arm temperature with respect to time is generated numerically using the forward difference approximation, with appropriate smoothing applied to both the original arm time series and the resulting derivative. Subsequently, it was found that near zero innovations could only be obtained by additionally *lagging* the correction term :

$$T_{ref}(t) = T_{arm}(t) + c_1\int_0^T c_2 e^{-\tau/\sigma}\frac{dT_{arm}}{dt}(t-\tau)d\tau \tag{3}$$

Where c_2 normalises the exponential lagging function over the interval $\tau = 0 \rightarrow T$. T is typically 30 minutes. σ defines the width of the lagging function and typically takes values in the range 2 - 10 minutes.

The effective emissivities of each channel and the scale factor (c_1) used to scale the correction term in equation 3 were determined by fitting the innovations for a single assimilation cycle. As an example, the results for the sounding channels 2 - 7 are shown in Figure 4. The apparent polarisation dependence of the effective emissivity

is illustrated by the difference between channels 2 - 5 (emissivities close to 0.01) and channels 6 and 7 (effective emissivities close to 0.02). It was found that for the SSMI-like imaging channels the effective emissivity is close to 0.00 and for the 183 GHz channels is in the range 0.035 - 0.045. Due to greater uncertainties in the background fields for the quantities influencing these channels and the greater uncertainties in the radiative transfer modelling for these channels the reproducibility of the results obtained using this technique is worse than for the lower atmopspheric sounding channels.

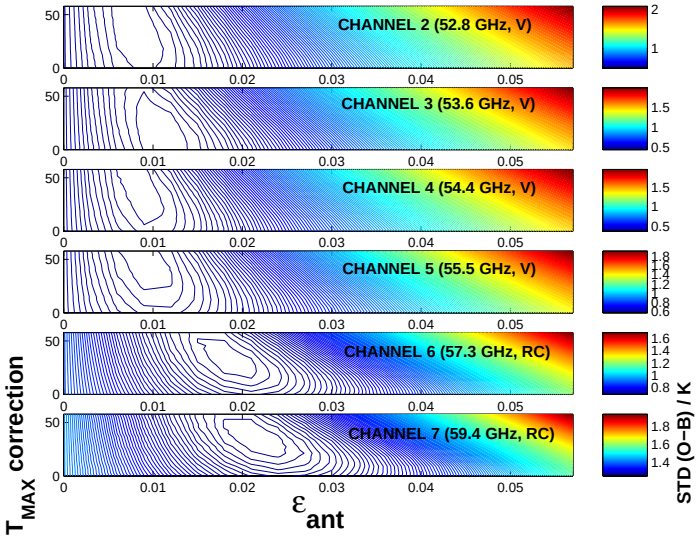

Figure 4: Contour plots showing the quality of fit, as measured by the stdev of (O - B) obtained for a range of assumed emissivities and maximum magnitude of the temperature corrections for channels 2 - 7

The physical basis for the empirical reflector emission correction can be investigated by considering the heat transfer equation governing the time evolution of the measured arm temperature:

$$a_1 \frac{dT_{arm}}{dt} = a_2 f(t) - a_3 (T_{arm}^n - T_0^n) \tag{4}$$

Where $f(t)$ captures the time evolution of the solar radiative forcing function, and the second term on the RHS is a *sink* term where n takes the value of 1 if the arm cools conductively to a sink at temperature T_0, and takes the value 4 if the dominant cooling mechanism is radiative. The constants $a_{1,2,3}$ are related to the heat capacity, geometry and thermal conductivity/emissivity of the arm respectively. During the part of the orbit where the spacecraft is in Earth shadow, the solar radiative forcing term is zero and the numerically computed derivative ($\frac{dT_{arm}}{dt}$) can be plotted against T_arm^n for the values $n = 1, 4$. Figure 5 shows the resulting plot for $n = 1$. From this it can be concluded that the arm temperature cools conductively ($n = 1$) to a sink at a temperature of approximately 217K. Equation 4 can then be rearranged to express the (scaled) solar forcing as follows:

$$\frac{a_2}{a_3} f(t) = (T_{arm} - T_0) + \frac{a_1}{a_3} \frac{dT_{arm}}{dt} \tag{5}$$

Therefore a scaled representation of the radiative forcing throughout the orbit can be constructed from the arm temperature data. The form of this derived forcing function is shown in Figure 6. There is good qualitative agreement between the form of this solar forcing and the form computed based on the spacecraft and orbit geometry, particularly in the regions prior to the spacecraft entering Earth shadow and immediately following emergence from Earth shadow.

If it can be assumed that the reflector also cools conductively, then the problem of determining the reflector

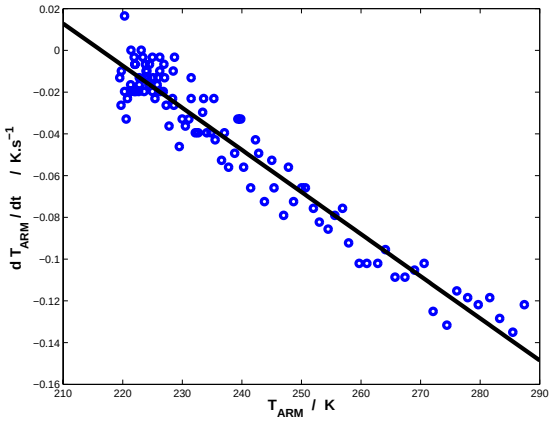

Figure 5: $\frac{dT_{arm}}{dt}$ *versus* T_{arm} *during earth shadow demonstrating that the arm cools conductively.*

arm temperature reduces to determining the solution of an equation similar to equation 4, with the forcing term given by equation 5

$$b_1 \frac{dT_{ref}}{dt} = b_2 f(t) - b_3(T_{ref} - T_0) \tag{6}$$

As the constants b_1,b_2 and b_3 , are related to the (unknown) thermal properties of the reflector it is not possible at this time to compute the solutions to equation 6 , but it can be solved numerically by fitting the form of solution to that given by the empirical temperature correction, in order to demonstrate that the empirical form of the reflector temperature is consistent with the solution of the heat transfer equation for *some* choice of thermal properties. A comparison of the derived reflector temperatures for both empirical and physical approaches in shown in Figure 6. The difference between the two forms is mostly within the 5K accuracy requirement but there is a discontinuity resulting from correctable residual edge effects in the empirical correction. Work is ongoing to reconcile these estimates of the antenna temperature with a fully physical solution to 6 based on reasonable estimates of the thermal properties of the reflector.

3.3 Other Approaches

The instrument manufacturers, in conjunction with the Cal/Val team have devised a gain correction scheme based on Fourier filtering the gains for each orbit. By discarding the high frequency components it is possible to determine the underlying true variation in the gain and determine the form of the intrusions. This scheme is currently being evaluated at NRL.

4 Performance

The performance of the instrument corrections has been assessed by monitoring the corrected radiances against Met Office background fields. A times series of innovations for channels 2, 3 and 4 is shown in Figure 7. The discontinuities are due to an upgrade to the operational forecast model (August 17th 2005) and implementation of the predictor based bias corrections in late September 2005. The standard deviations of the innovations during this time are in the range 0.2 - 0.3K for channels 2, 3 and 4.

An examination of the analysis increments shows that the corrections are not yet optimally tuned. Nevertheless, baseline forecast impact trials carried out at ECMWF using only the SSMIS temperature sounding channels

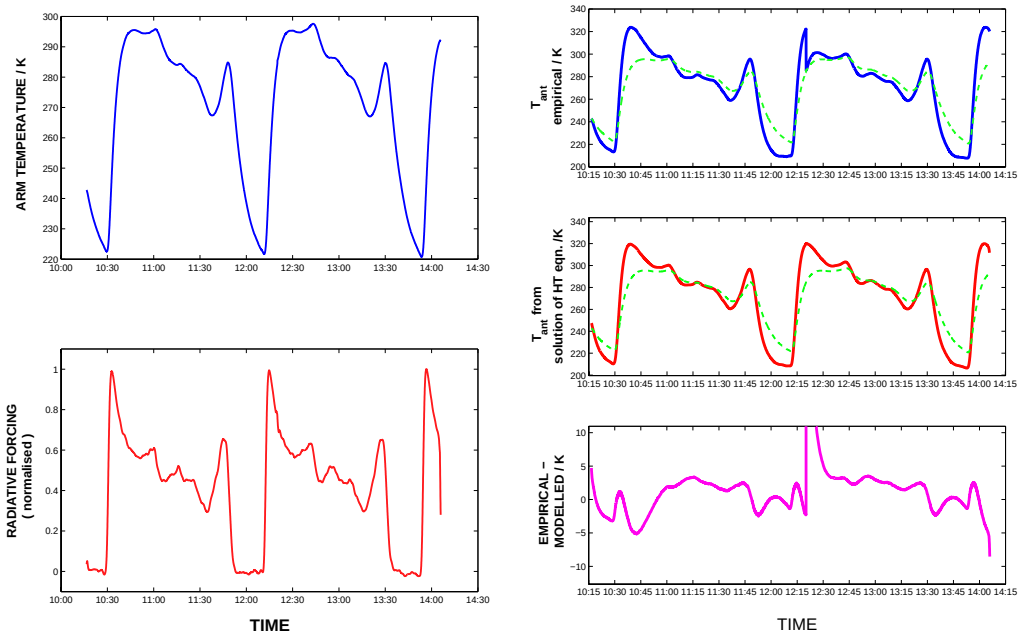

Figure 6: The form of the derived radiative forcing (left) and a comparison of the numerical solution of the heat transfer equation governing the evolution of the reflector temperature (right, red curve) with the empirically derived reflector temperature (right, blue curve) and the difference (right, green). The measured arm temperature is indicated in green dashes.

show the impact of the pre-processed SSMIS data to be more than 50% of the impact of NOAA 15 AMSU-A in the southern hemisphere against control runs in which no satellite data was assimilated. The anomaly correlation plots for geopotential height at 500 hPa for both hemispheres are shown in Figure 8. In a second set of impact trials, the addition of SSMIS on top of the full operationally assimilated dataset gave impacts which were neutral - slightly negative.

5 Future Prospects

The experience and insight gained during the extended Cal/Val period for F16 SSMIS has facilitated the development of software mitigation strategies to deal with several sources of instrument bias described here. The best correction algorithms developed at NRL, the Met Office, NOAA and by the instrument manufacturer will be incorporated in a pre-processor to be run at Fleet Numerical Meteorological Operations Centre (FNMOC) to produce radiances for radiance assimilation applications. It is expected that this data stream will become available sometime in 2006.

Hardware modifications are in place for F17 SSMIS which should significantly reduce the impact of the direct solar intrusions on the warm load. The temperature sensor on the F17 SSMIS reflector has been re-sited to the back of the main reflector, on the reflector substrate. It is at this stage unclear at this stage whether this will permit more accurate estimation of the reflector temperature. Laboratory measurements of reflector material give emissivity measurements lower (by a factor of 10) than those empirically derived here. It is possible, therefore, that the degradation of the main reflector surface prior to launch is unique to F16 SSMIS and that reflector emission will be a less significant effect for future sensors.

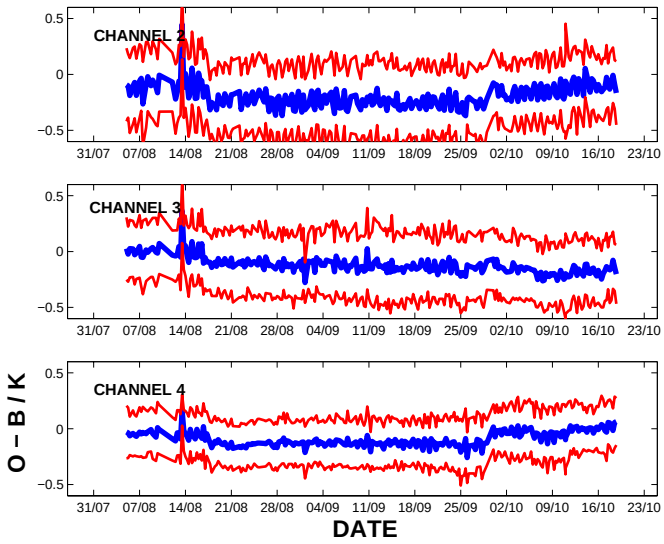

Figure 7: Radiance monitoring plots for SSMIS channels 2,3 and 4 for the period August - October 2005. Mean bias (blue) and standard deviation (red) are shown and are in the range 0.2 - 0.3 K. The main discontinuities arise from a change to the operational global model (17th August 2005) and implementation of a second stage bias correction on 27th September 2005.

6 Conclusions

The extended Cal/Val phase following the launch of F16 SSMIS highlighted a number of serious instrument problems. Two tools have been particularly useful in diagnosing the cause of these problems: the use of NWP background fields from which scan averaged innovation timeseries can be generated and a visualisation package using engineering CAD data in conjunction with orbital data to accurately model the orientation of the instrument components in space. Based on the insights gained, physically based correction algorithms have been developed. These algorithms are currently under test at NRL, NOAA and the Met Office. Initial forecast impact studies based on preliminary pre-processed data have shown significant positive impact on forecast quality relative to controls using no satellite data. The impact is close to the impact of NOAA 15 AMSU data and further improvements in data quality and coverage are expected in the near future as the corrections are tuned further and the moisture sounding and imaging channels are incorporated.

The launch of F17 SSMIS is currently scheduled for June - December 2006. If the additional impact on forecast impact is realised, SSMIS should become an important data source for NWP assimilation systems over the next 10 years.

Acknowledgements

The authors would like to thank Brett Candy, Fiona Hilton, Andrew Smith and Nigel Atkinson for their contribution to the development of the generic radiance processing system at the Met Office, John Eyre for helpful discussions, and finally the organisers of and participants in the *SSMIS mini-workshop on radiance assimilation* held at NRL, Monterey, during October 2005.

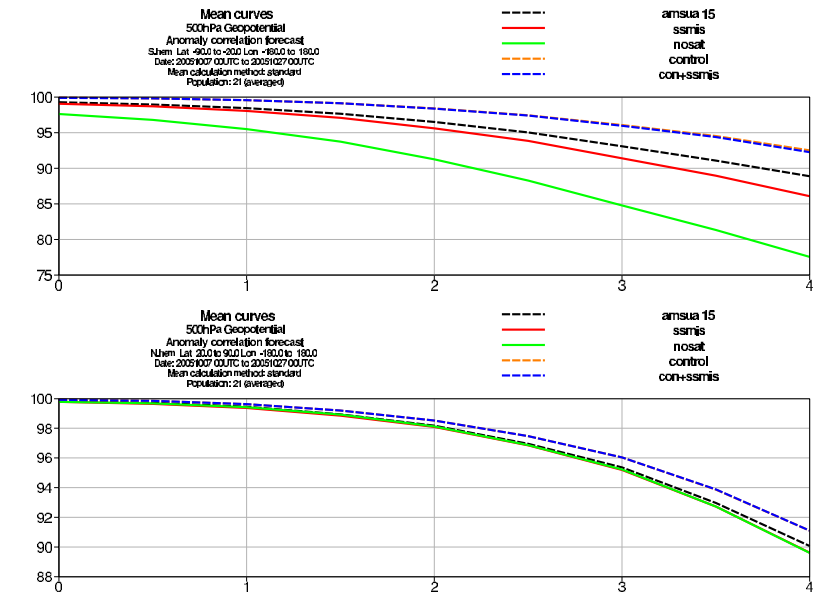

Figure 8: Anomaly correlation plots for geopotential height at 500 hPa in NH (top) and SH (bottom).

References

Atkinson, N., J. Cameron, B. Candy and S.J. English (2005), Bias Correction of Satellite Data at the Met Office, (these proceedings)